Characterization of metal contacts for two-dimensional MoS_2 nanoflakes

Characterization of metal contacts for two-dimensional MoS_2 nanoflakes

Sumeet Walia,[1,2,a)] Sivacarendran Balendhran,[1,2] Yichao Wang,[2] Rosmalini Ab Kadir,[2] Ahmad Sabirin Zoolfakar,[2] Paul Atkin,[2] Jian Zhen Ou,[2] Sharath Sriram,[1,2] Kourosh Kalantar-zadeh,[2,a)] and Madhu Bhaskaran[1,2,a)]
[1]*Functional Materials and Microsystems Research Group, RMIT University, Melbourne, Victoria 3000, Australia*
[2]*School of Electrical and Computer Engineering, RMIT University, Melbourne, Victoria 3000, Australia*

(Received 29 October 2013; accepted 17 November 2013; published online 4 December 2013)

While layered materials are increasingly investigated for their potential in nanoelectronics, their functionality and efficiency depend on charge injection into the materials *via* metallic contacts. This work explores the characteristics of different metals (aluminium, tungsten, gold, and platinum) deposited on to nanostructured thin films made of two-dimensional (2D) MoS_2 flakes. Metals are chosen based on their work functions relative to the electron affinity of MoS_2. It is observed, and analytically verified that lower work functions of the contact metals lead to smaller Schottky barrier heights and consequently higher charge carrier injection through the contacts.
 [http://dx.doi.org/10.1063/1.4840317]

Two-dimensional (2D) materials are gaining significant attention due to their unique electrical, mechanical, and optical properties, which are different than those of their bulk counterparts.[1,2] In particular, 2D transition metal dichalcogenides are attracting extensive research interest due to possibilities of electronic band structure manipulations.[1,2] Amongst them, molybdenum disulphide (MoS_2) which is a n-type semiconductor, has been the most popular material owing to its relatively small bandgap (1.2 eV for multi-layer and 1.8 eV for monolayer), modest electron mobilities and transition from indirect to direct bandgap when it is exfoliated to monolayer thickness.[1,2] Amidst the three known polymorphs of MoS_2 (1T, 2H, and 3R), 2H-MoS_2 is the naturally occurring and thermodynamically stable phase.[1,2] Bulk 2H-MoS_2 is composed of atomically thin planes comprising of covalently bonded S–Mo–S structures across the planes and weak van der Waals forces between the planes.[3] Such a crystal structure enables the realisation of atomically thin stable 2D sheets of MoS_2 *via* mechanical and liquid exfoliation techniques.[1,2]

2D MoS_2 has been applied in the development of a variety of devices including field effect transistors, electrically driven optical devices and solar cells, as well as electrochemical devices.[4–6] All these devices rely on electrical contacts for their operation. As such, understanding metal/2D MoS_2 interface is crucial in such devices and the nature of the metal/2D MoS_2 depends on the electronic band structures of both the metal and 2D MoS_2.

In this letter, we provide a thorough experimental analysis of metal/nanostructured thin films made of 2D MoS_2 nanoflakes contacts for selected metals. The choice of metal contacts is based on their work functions (Φ_M) relative to the electron affinity (χ) of MoS_2. Relatively low work function metals, aluminium (Al) and tungsten (W), are studied along with relatively high work function metals, gold (Au) and platinum (Pt), in order to provide a wide-ranging picture of the behaviour of the metal/2D MoS_2 contacts.

In this study, a grinding-sonication liquid exfoliation technique, adapted from the work of Yao *et al.*,[7] is employed as a high yield method for producing suspensions of 2D MoS_2 nanoflakes.[8] Atomic force microscopy (AFM) was employed to assess the thickness of the MoS_2 nanoflakes. It can be seen from Fig. 1(a) that typical MoS_2 nanoflakes comprise of 6 to 8 fundamental layers (1 layer = 0.65 nm).[4] Measurements using a large number of AFM images show that the majority of MoS_2 nanoflakes exhibit thicknesses in the range of 2–7 monolayers.[9] Dynamic light scattering (DLS) analysis was conducted to assess the average lateral dimensions of the exfoliated nanoflakes (Fig. 1(b)) to be approximately 100 nm. The nanoflake suspension was drop-casted onto electrically conductive fluorine-doped tin oxide (FTO) substrates and left to dry under ambient conditions, resulting in thin films of ~500 nm thickness.

Raman spectroscopy was carried out to further characterise the MoS_2 thin films and estimate the number of layers, they are comprised of. Figure 2(a) shows the Raman spectra of the bulk and the nanostructured MoS_2 thin film. The two dominant modes (E^1_{2g} and A_{1g}) reflect the vibrations of the Mo–S bond along the horizontal and vertical planes, respectively.[10] For the MoS_2 nanoflakes, the A_{1g} mode showed no significant shift, while the E^1_{2g} mode was observed to have red shifted in comparison to their bulk counterpart. This indicates a dominant presence of few-layered (<7 layers) MoS_2 nanoflakes in the thin film,[9,11] which is also in agreement to the AFM analysis presented earlier.

X-ray diffraction (XRD) was utilized to determine the crystallinity of the drop-casted 2D MoS_2 nanostructured thin films. It can be seen from Fig. 2(b) that the dominant peak reflecting the (002) plane (ICDD Card no: 77–1716) was observed at 14.4°. In contrast to the XRD pattern of the bulk MoS_2, the nanostructured MoS_2 thin film did not reveal the presence of (100), (106), (006), (105), and (008) planes. This reflects the nature of the thin films which consist of 2D MoS_2 nanoflakes composed of mostly (002) planes.

[a)]Authors to whom correspondence should be addressed. Electronic addresses: madhu.bhaskaran@rmit.edu.au, kourosh.kalantar@rmit.edu.au, and sumeet.walia@rmit.edu.au

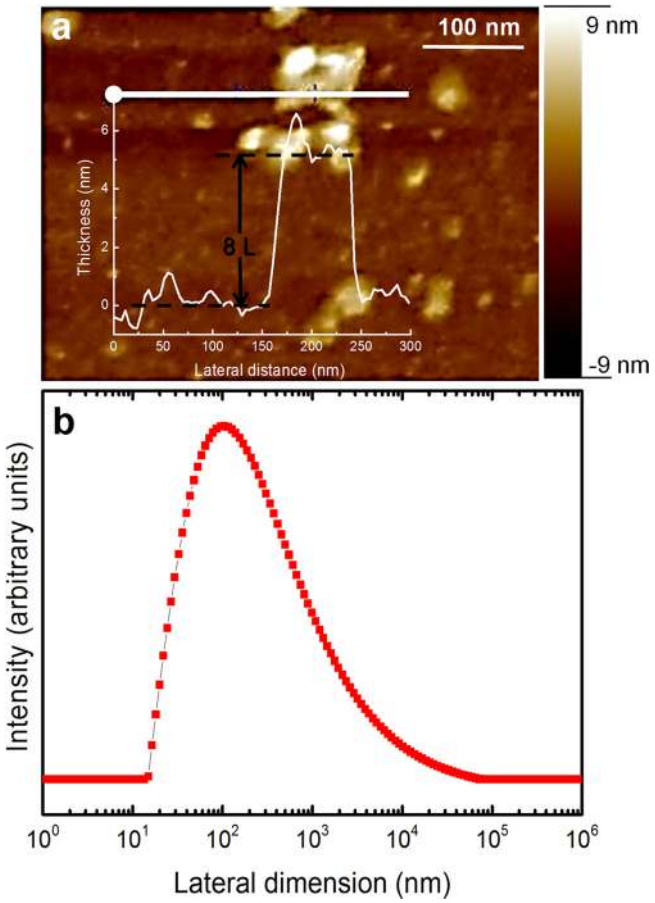

FIG. 1. (a) AFM image of typical exfoliated MoS_2 nanoflakes with its corresponding cross-sectional thickness profile. (b) DLS analysis of the lateral size distribution of the MoS_2 nanoflakes.

High resolution transmission electron microscopy (HRTEM) was conducted in order to verify the crystal structure of the 2D MoS_2 nanoflakes. The HRTEM image of the edges of the nanoflakes (Fig. 2(c)) confirms the presence of 2D structures with only several fundamental layers. The inset of Fig. 2(c) shows that the parallel lattice fringes of the MoS_2 nanoflakes are 0.27 nm apart, which is in agreement with previously reported values for 2H-MoS_2.[1]

In order to investigate the properties of metals when contacted with nanostructured films made of 2D MoS_2 nanoflakes, four different metals of Al, W, Au, and Pt with varying work functions were considered. Al ($\Phi_{Al} = 4.54$ eV)[12] and W ($\Phi_W = 5.09$ eV)[12] were chosen as the low work function metals, while Au ($\Phi_{Au} = 5.40$ eV)[12] and Pt ($\Phi_{Pt} = 5.70$ eV)[12] were chosen as the high work function metals, relative to the electron affinity of MoS_2 ($\chi = 4.0$ eV).[6,13] A band diagram illustration of all the aforementioned metals relative to MoS_2, prior to contact is shown in Fig. 3(a). Figure 3(b) shows the current-voltage (I-V) characteristics acquired for the different metal/MoS_2 contacts. It can be seen that Al/MoS_2 interface results in the highest current ($\sim$90 μA), while the Pt/MoS_2 interface shows the least current ($\sim$10 μA), under identical bias conditions.

When the metal and the MoS_2 are brought in a contact, the bands of MoS_2 bend such that the Fermi levels equilibrate. Figure 4(a) schematically illustrates the respective electronic band alignment of the metals for the case of

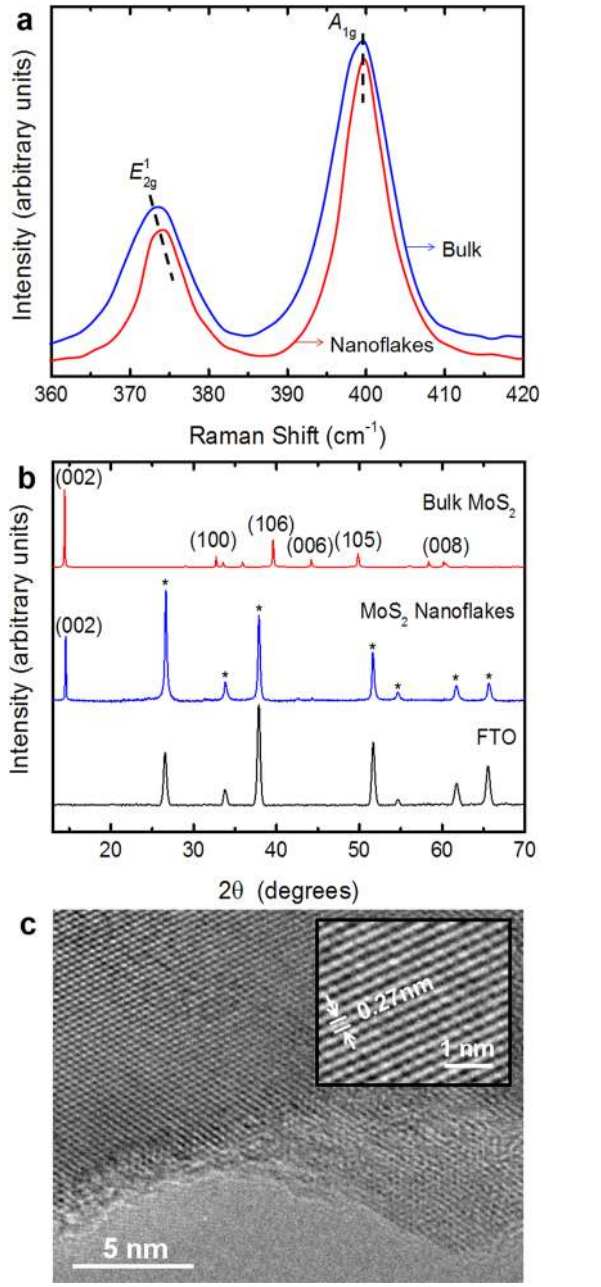

FIG. 2. (a) Raman spectra comparison of bulk MoS_2 and a nanostructured 2D MoS_2 thin film. (b) X-ray diffractograms comparing bulk MoS_2 powder, a nanostructured thin film made of 2D MoS_2 nanoflakes, with the FTO substrate spectrum provided for reference (* denotes the peaks corresponding to the FTO substrate). (c) Transmission electron micrograph of a liquid exfoliated 2D MoS_2 nanoflake with the inset corresponding to its high resolution transmission electron micrograph.

$\Phi_M > \chi$ (in our case, the Φ_M of Al, W, Au, and Pt all are larger than χ), before the metal and MoS_2 and brought into contact. On making contact, the conduction and valence bands of the MoS_2 bend in order to achieve equilibrium between the metal Fermi level and the MoS_2 chemical potential (4.36 eV).[14] The degree and the direction of band bending depend on the work function of the metal relative to the Fermi level of the semiconductor (MoS_2 in this case). With MoS_2 as the n-type semiconductor and for the case, where the metal work function is larger than the electron affinity of MoS_2, the depiction shown in Fig. 4(b) arises after the metal and semiconductor are brought into contact. In this case, the

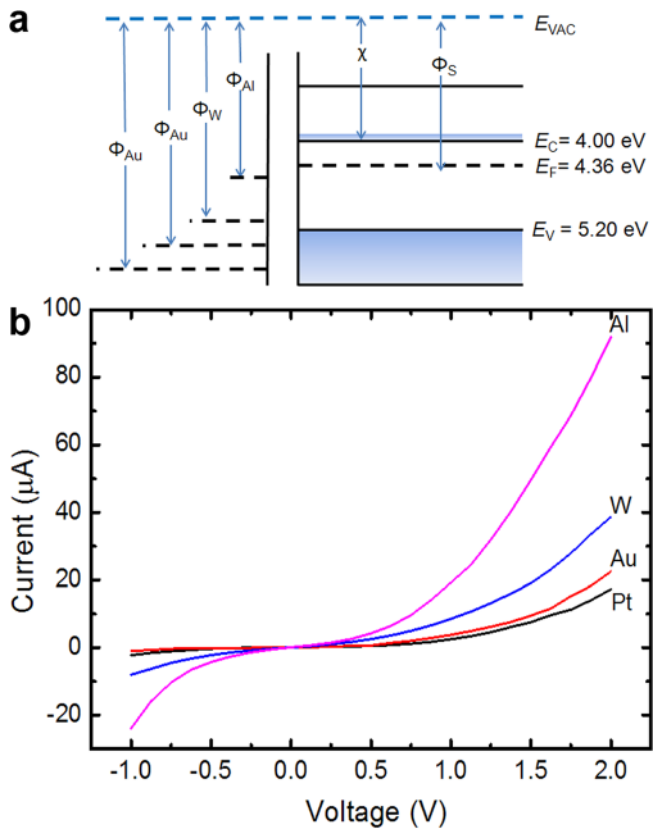

FIG. 3. (a) Band diagram illustrations of a metal and MoS_2. χ is the MoS_2 electron affinity, E_F is the Fermi level of MoS_2, E_{VAC} is the reference vacuum level, E_V and E_C are the valence and the conduction band levels, respectively. (b) *I-V* characteristics for different metal/MoS_2 contacts under identical bias conditions.

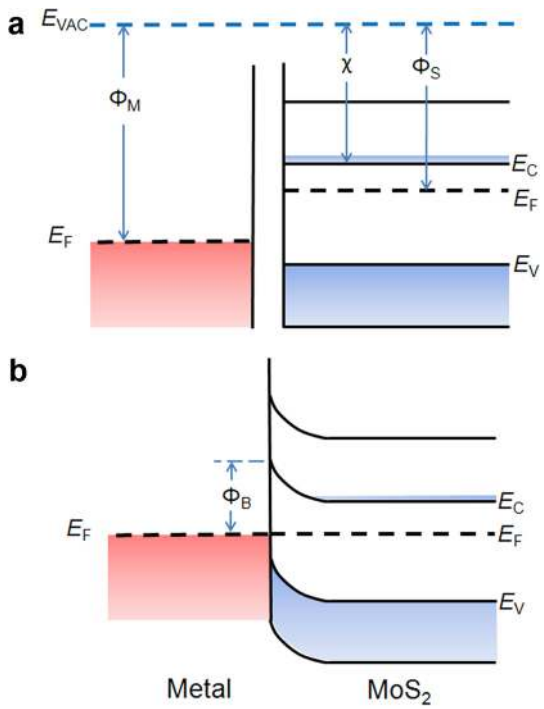

FIG. 4. Band alignments of a metal and MoS_2 for $\Phi_M > \chi$ (a) before establishing a contact and (b) their corresponding band bending after establishing a contact.

TABLE I. Performance summary of different metal/2D MoS_2 contacts.

Metal	Work function, Φ_M (eV)	Schottky barrier height, $\Phi_B = \Phi_M - \chi$ (eV)	Current at +2 V bias (μA)
Al	4.5	0.5	91.9
W	5.1	1.1	38.7
Au	5.4	1.4	22.5
Pt	5.7	1.7	17.3

electrons diffuse from the semiconductor to the lower energy states of the metal in order to achieve a constant Fermi level throughout the system in thermal equilibrium. This results in the upward band bending within MoS_2 at the interface. Consequently, the electrons in the metal see a potential barrier against their migration into the semiconductor. This barrier is known as the Schottky barrier (Φ_B), which can be estimated by the Schottky-Mott rule ($\Phi_B = \Phi_M - \chi$), where χ is the electron affinity of the semiconductor). A higher Φ_M thus results in a higher Φ_B. Hence, a larger forward bias is required in order to overcome this Schottky barrier.

This is confirmed from the *I-V* characteristics (Fig. 3(b)), in which it is seen that the current is progressively higher for lower work function metals such as Al and W under identical bias conditions. Table I summarises the experimental results obtained using different metal contacts with varying work functions, relative to the electron affinity of MoS_2. This shows that Al (the lowest work function metal) results in the highest bias current, indicating its superior room temperature charge injection capabilities for an interface with MoS_2, compared to commonly used contact metals such as Au and Pt. The estimated Schottky barrier heights using the Schottky-Mott relationship are shown in Table I. We also calculated the Schottky barrier heights from the *IV* curves. The calculated Φ_B for Al (0.55 eV) corresponds well to the theoretically estimated value. However, an accurate calculation for the other metals could not be obtained, as their relatively large Φ_B required the application of higher bias voltages, causing the junction to break down.

In summary, we investigated the properties of the metal/2D MoS_2 contacts using metals of different work functions and demonstrated that for the chosen metals that have the work functions between 4.5 to 5.7 eV, always Schottky behaviours were observed. While, there are reports in literature that have claimed the Au/2D MoS_2 contact to be Ohmic, our study clearly shows the formation of a barrier height and therefore Schottky behaviour for all of the metals under investigation. This study showed that the choice of the metal contacts is crucial in adjusting the barrier heights at their interface with 2D MoS_2, which is fundamental knowledge in designing electronic and optoelectronic devices based on 2D MoS_2.

The authors acknowledge support from the Australian Research Council (ARC) with project support through Discovery Project No. DP130100062 and DP140100170; Australian Post-Doctoral Fellowships through Discovery Project Nos. DP1092717 (MB) and DP110100262 (SS); and equipment funding through the Linkage, Infrastructure, Equipment, and Facilities Grant No. LE100100215 (SS and KKZ). S.B. acknowledges a publication grant from the School of Graduate Research at RMIT University.

[1]S. Balendhran, S. Walia, H. Nili, J. Z. Ou, S. Zhuiykov, R. B. Kaner, S. Sriram, M. Bhaskaran, and K. Kalantar-zadeh, Adv. Funct. Mater. **23**, 3952 (2013).
[2]Q. H. Wang, K. Kalantar-Zadeh, A. Kis, J. N. Coleman, and M. S. Strano, Nat. Nanotechnol. **7**, 699 (2012).
[3]D. J. Late, B. Liu, H. S. S. Ramakrishna Matte, V. P. Dravid, and C. N. R. Rao, ACS Nano **6**, 5635 (2012).
[4]B. Radisavljevic, A. Radenovic, J. Brivio, V. Giacometti, and A. Kis, Nat. Nanotechnol. **6**, 147 (2011).
[5]H. Wang, L. Yu, Y.-H. Lee, Y. Shi, A. Hsu, M. L. Chin, L.-J. Li, M. Dubey, J. Kong, and T. Palacios, Nano Lett. **12**, 4674 (2012); Z. Yin, H. Li, H. Li, L. Jiang, Y. Shi, Y. Sun, G. Lu, Q. Zhang, X. Chen, and H. Zhang, ACS Nano **6**, 74 (2012); G. Eda, H. Yamaguchi, D. Voiry, T. Fujita, M. Chen, and M. Chhowalla, Nano Lett. **11**, 5111 (2011).
[6]S. Das, H.-Y. Chen, A. V. Penumatcha, and J. Appenzeller, Nano Lett. **13**, 100 (2013).
[7]Y. Yao, L. Tolentino, Z. Yang, X. Song, W. Zhang, Y. Chen, and C. P. Wong, Adv. Funct. Mater. **23**, 3577 (2013).
[8]See supplementary material at http://dx.doi.org/10.1063/1.4840317 for experimental details outlining the materials and methods used in this work.
[9]Y. Wang, J. Z. Ou, S. Balendhran, A. F. Chrimes, M. Mortazavi, D. D. Yao, M. R. Field, K. Latham, V. Bansal, J. R. Friend, S. Zhuiykov, N. V. Medhekar, M. S. Strano, and K. Kalantar-zadeh, "Electrochemical control of photoluminescence in two-dimensional MoS_2 nanoflakes," ACS Nano **7**, 10083 (2013).
[10]S. Balendhran, J. Z. Ou, M. Bhaskaran, S. Sriram, S. Ippolito, Z. Vasic, E. Kats, S. Bhargava, S. Zhuiykov, and K. Kalantar-Zadeh, Nanoscale **4**, 461 (2012).
[11]D. J. Late, B. Liu, H. S. S. Ramakrishna Matte, C. N. R. Rao, and V. P. Dravid, Adv. Funct. Mater. **22**, 1894 (2012).
[12]H. L. Skriver and N. M. Rosengaard, Phys. Rev. B **46**, 7157 (1992).
[13]K. Lee, H. Y. Kim, M. Lotya, J. N. Coleman, G. T. Kim, and G. S. Duesberg, Adv. Mater. **23**, 4178 (2011).
[14]J.-M. Yun, Y.-J. Noh, J.-S. Yeo, Y.-J. Go, S.-I. Na, H.-G. Jeong, J. Kim, S. Lee, S.-S. Kim, and H. Y. Koo, J. Mater. Chem. C **1**, 3777 (2013).